Journal of Applied Polymer Science

Poly(ε-caprolactone)/polyhedral oligomeric silsesquioxane hybrids: Crystallization behavior and thermal degradation

Sainan Xia,[1] Qingsheng Liu,[1,2] Ying Shen,[1] Pengfei Yao,[1] Bingyao Deng[1]
[1]Key Laboratory of Eco-Textiles, Ministry of Education, Jiangnan University, Wuxi, 214122, China
[2]Key Laboratory of Yarn Materials Forming and Composite Processing Technology, Zhejiang Province, China
Correspondence to: Q. Liu (E-mail: qsliu@jiangnan.edu.cn) and B. Deng (E-mail: bydeng168@163.com)

ABSTRACT: Biodegradable organic–inorganic hybrids based on poly(ε-caprolactone) (PCL) and polyhedral oligomeric silsesquioxane (POSS) with 5.3–21.3 wt % POSS were synthesized via ring-opening polymerization (ROP). Chemical structures of the polymers were characterized by proton nuclear magnetic resonance (^{1}H NMR), fourier transform infrared spectroscopy (FTIR), and gel permeation chromatography (GPC). X-ray diffraction (XRD) analysis illustrated that both POSS and PCL segment in POSS/PCL hybrids could crystallize and form two well-separated crystalline phases except in the one with low content of POSS (5.3 wt %). Melting behavior and non-isothermal crystallization kinetics of POSS/PCL hybrids were studied by differential scanning calorimeter (DSC). The results indicated that the POSS segment suppressed crystallization of the PCL segment to some extent. Polarizing optical microscope (POM) images showed that POSS/PCL hybrids with the highest POSS loading (21.3 wt %) possessed "snowflake" shape crystals whereas the ones with relatively low POSS loading exhibited classic spherulites. Thermogravimetry (TG) measurement revealed that thermal degradation of POSS/PCL hybrids proceeded by four-step while PCL homopolymers degraded by a single step. © 2016 Wiley Periodicals, Inc. J. Appl. Polym. Sci. **2016**, *133*, 44113.

KEYWORDS: composites; copolymers; crystallization; differential scanning calorimetry (DSC); properties and characterization

Received 22 March 2016; accepted 20 June 2016
DOI: 10.1002/app.44113

INTRODUCTION

Poly(ε-caprolactone) (PCL) is a kind of aliphatic polymer. It has been widely explored for biomedical field due to its biodegradability, biocompatibility, and processibility. However, PCL has been limited to diverse application because of its low mechanical properties and long-term degradation.[1,2] Thus, considerable research on modification of PCL have been conducted to overcome its performance defects. Among various modification methods, introduction of polyhedral oligomeric silsesquioxane (POSS) into polymer backbone allows the organic and inorganic phase to interact at the molecular level[3] and can obtain organic–inorganic hybrids. POSS itself is a hybrid material.[3] A typical POSS molecule possesses an inorganic silica-like core (Si_8O_{12}), which is surrounded by a shell of eight organic reactive or non-reactive corner groups.[3–6] The reactive groups such as amino and hydroxyl are able to introduce POSS into polymer matrix by covalent connection. The covalent connection can limit aggregation of POSS units, improving dispersion of POSS in polymer matrix in contrast to physical blending. Inclusion of POSS within PCL matrix leads to remarkable potential properties, and it also enhances thermal stability, biostability, mechanical properties, and oxidative resistance of polymer.[3,4,7,8]

POSS-containing PCL hybrids have been extensive investigated. For instance, Mirmohammadi *et al.*[7,8] prepared PCL/POSS and poly(ε-caprolactone fumarate) (PCLF)/POSS nanohybrids via anionic ring opening polymerization and *in situ* photocrosslinkable, respectively, and then studied their thermal and mechanical behavior. Fernández *et al.*[9] synthesized POSS-containing PCL hybrids via click coupling between alkyen moiety-functionalized POSS and bis-azide end-functionalized PCL and investigated their thermal degradation behavior and surface properties. Liu *et al.*[6] and Mya *et al.*[10] synthesized star-shaped POSS/PCL hybrids. The Mather and coworkers[3,11] prepared TMP diollsobutyl-POSS/PCL nanocomposites and further synthesized POSS/PCL networks. The authors focused on their shape memory properties, microstructure, and phase behavior. In this article, we synthesized the same hybrids based on TMP diollsobutyl-POSS and PCL and studied their non-isothermal crystallization behavior and thermal degradation process. In our work, Mo equation was used to describe non-isothermal crystallization kinetics of POSS/PCL hybrids and PCL homopolymers. The thermal decomposition process of POSS/PCL hybrids and

Additional Supporting Information may be found in the online version of this article.

pure PCL were studied by thermal gravimetric analyzer (TGA). In addition, crystalline morphologies of POSS/PCL hybrids were investigated by hot-stage polarizing microscope (HSPOM).

EXPERIMENTAL

Material Preparation

TMP Diollsobutyl-POSS was produced from Hybrid Plastics Co., Hattiesburg, Mississippi, US. ε-Caprolactone (ε-CL) (>99%) was supplied from J&K Scientific Co. Ltd., Beijing, China. Chloroform, dibutyltin dilaurate (>90%), deuterated chloroform ($CDCl_3$), ethylene glycol (EG), and tetrahydrofuran (THF, LC grade) were purchased from Guoyao Group Chemical Reagent Co. Ltd., Shanghai, China. Ethanol (>99.7%) was obtained from Shanghai Titan Scientific Co. Ltd., Shanghai, China. All reagents were used as received without further purification.

Synthesis of Pure PCL and POSS/PCL Hybrids

The POSS and EG were separately used as initiators to initiate ring-opening polymerization (ROP) of ε-CL in the presence of dibutyltin dilaurate, which served as a catalyst. For example, 17.80 mL (0.5 mol) of ε-CL, 17.77 g (16.7 mmol) of POSS, and 10 drops of dibutyltin dilaurate were added into a 250 mL flask under a nitrogen atmosphere, and the mixture was stirred at 140 °C for 16h. The resulting polymers were dissolved in chloroform and precipitated into excess ethanol to remove residual ε-CL, POSS, and catalyst. The precipitations were filtered and dried in a vacuum oven at 40 °C for 48 h. POSS/PCL hybrids and pure PCL with varying molecular weight were obtained by adjusting the molar ratio of POSS or EG to ε-CL.

Gel Permeation Chromatography (GPC)

The molecular weight (M_n) and polydispersity index (PDI) of the samples were characterized by Waters 1515 HPLC. The instrument was equipped with Styragel HR 2 THF column and Styragel HR 4 THF column (7.8 mm × 300 mm). Polystyrene standards were used for calibration. The samples were dissolved in tetrahydrofuran at a concentration of 6.0 mg/mL and then run with a flow rate of 1.0 mL/min at 35 °C.

Fourier Transform Infrared Spectroscopy (FTIR)

Fourier transform infrared spectra (4,000–400 cm^{-1}) of the samples were acquired employing Nicolet iS10 FTIR and using KBr disk method. Each spectrum was recorded with a total of 16 scans; each had a resolution of 4 cm^{-1} at room temperature.

Nuclear Magnetic Resonance (NMR)

Proton NMR (^1H NMR) spectra were recorded using Bruker Aduance III 400 MHz system, operating at 400.13 MHz. In all, 16 scans were acquired and the delay time was 0.006 s. Each sample was dissolved in $CDCl_3$ with a concentration of about 87.5 mg/mL and then detected at room temperature.

X-ray Diffraction (XRD)

Crystal structures of the samples were detected by Bruker D8 diffraction system with Cu K_α ($\lambda = 1.5406$ Å) radiation source. The measurements were made at a voltage of 40 kV and a current of 40 mA. Scans were run from a 2θ value of 5 to 60° at a scan speed of 4°/min.

Differential Scanning Calorimeter (DSC)

The melting and crystallization behaviors and the non-isothermal crystallization kinetics of the samples were studied by DSC Q200. Nitrogen was used as the purge gas at the flow rate of 50 mL/min. The weight of the samples was in the range of 4–6 mg.

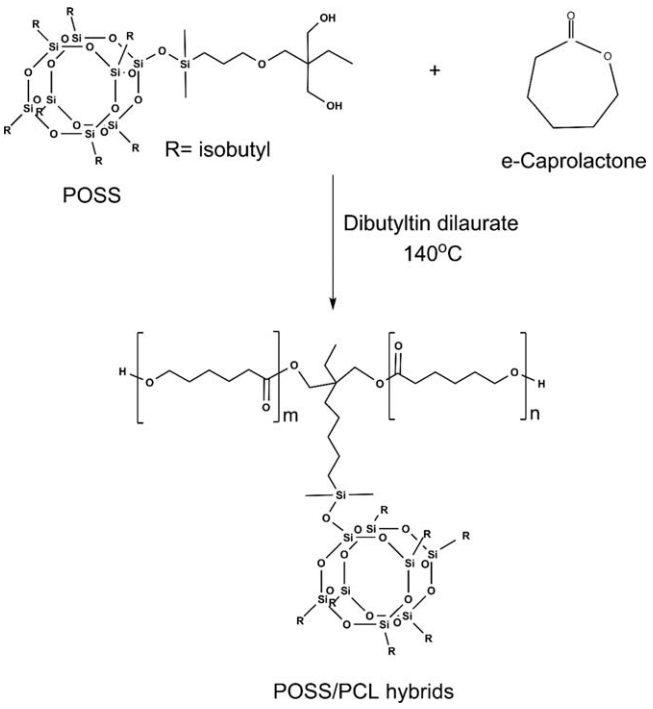

Figure 1. Synthesis of POSS/PCL hybrids.

Hot-Stage Polarizing Microscope (HSPOM)

Crystal morphologies of the samples were observed by Leica DM2700P, which was equipped with LINKAM TMS420 hot stage and a CCD camera. POSS/PCL hybrids were melted at 150 °C (100 °C for pure PCL) for 3 min and then quickly cooled to 40 °C in the hot-stage for isothermal crystallization.

Thermal Gravimetric Analyzer (TGA)

Thermal stability of the samples was characterized by TGR Q500. POSS and POSS/PCL hybrids were heated from 50 to 600 °C (500 °C for pure PCL) at the rate of 10 °C/min. The analyses were done in a nitrogen atmosphere at a flow rate of 60 mL/min.

RESULTS AND DISCUSSION

Preparation of POSS/PCL Hybrids and Pure PCL

POSS/PCL hybrids and pure PCL were synthesized by using TMP Diollsobutyl-POSS and EG as initiator to initiate ROP of ε-CL under the action of catalyst, dibutyltin dilaurate. Figure 1 described the synthesis process. POSS/PCL hybrids and pure PCL with different molecular weight were obtained. The resulting polymers were named PP10, PP30, PP120, EP10, EP30, and EP120, respectively. Here, 10, 30, and 120 denoted the molar ratio of ε-CL to initiator. The molecular weight and its distribution of pure PCL and POSS/PCL hybrids were characterized by GPC and the curves were presented in Figure 2. The curves of all samples were unimodal, indicating the pure polymers were obtained. It could be seen that the value of elution time of the hybrids and corresponding PCL homopolymers decreased with the molar ratio of ε-CL to hydroxyl group, indicating that

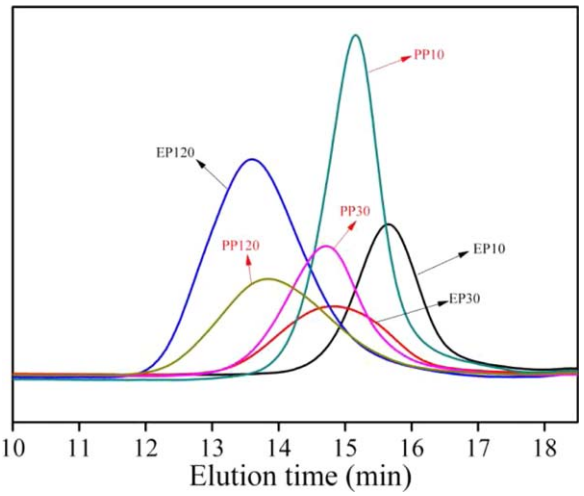

Figure 2. GPC traces of pure PCL and POSS/PCL hybrids. [Color figure can be viewed at wileyonlinelibrary.com.]

the molecular weight increased with the amount of ε-CL. Notably, EP30 and PP30 had nearly the same molecular weight, evidenced by the similar elution time. The molecular weight and its distribution of the samples were given in Table I.

Fourier Transform Infrared Spectroscopic (FTIR) Analysis

The FTIR spectra of the samples were shown in Figure 3. In Figure 3(a), the bands at 2,849 cm^{-1} and 2,868 cm^{-1} were assigned to methylene stretching vibration of PCL.[6,7,10,12] The sharp peak at 1,723cm^{-1} was considered as C═O stretching vibration of PCL.[7,10,12–14] The band near 1,189 cm^{-1} corresponded to C—O—C asymmetric stretching vibration of PCL and its symmetric stretching vibration appeared at 1,108 cm^{-1}.[10] Only characteristic peaks of PCL segment could be observed in the FTIR spectra of POSS/PCL hybrids. To determined characteristic peak of POSS segment of the hybrids, the bands at 1,300–900 cm^{-1} were shown in Figure 3(b). A shoulder near 1,108 cm^{-1} (denoted by arrow) was found in the FTIR spectra of the hybrids and it became obvious as POSS content increased. Meanwhile, as shown in Figure 3(a), the Si—O absorption band of pure POSS appeared at 1,113 cm^{-1}.[6,7,13] These results showed that the shoulder corresponded to Si—O absorption peak of the POSS segment and it slightly overlapped with the absorption band of C—O—C symmetric stretching vibration.

^{1}H NMR Analysis

Figure 4 presented ^{1}H NMR spectra of POSS, pure PCL, and POSS/PCL hybrid. In the spectrum of POSS/PCL hybrids, a new resonance peak appeared at j (3.28 ppm). The resonances at a (0.082 ppm), b (0.58 ppm), c + d (0.93), and h (1.83) were assigned to the POSS segment. The resonances at e (1.35 ppm), f + g (1.62 ppm), i (2.28 ppm), m (3.62 ppm), and k (4.04 ppm) were related to the PCL segment. The existence of resonance peaks of PCL and POSS demonstrated that POSS/PCL hybrids were synthesized successfully. From the ^{1}H NMR spectra of POSS/PCL hybrids, the POSS content was calculated and the results were listed in Table I.

XRD Analysis

The PCL homopolymers, POSS/PCL hybrids, and pure POSS were studied for crystal structure by X-ray diffraction (XRD) and the diffraction patterns were presented in Figure 5. The characteristic reflection peaks of pure POSS appeared at 8.12°, 10.8°, and 18.8°, corresponding to (101), (110), and (122) crystalline planes, respectively.[11] The diffraction patterns of PCL homopolymers revealed sharp reflection at 21.5°, 22.2°, and 23.9°, corresponding to (110), (111), and (200), respectively.[3,5,6,10,15] The POSS/PCL hybrids with high POSS content exhibited the crystalline planes for both POSS and PCL, indicating that the two crystalline phases coexisted in the hybrids. In addition, the characteristic peak intensity of POSS phase at 8.12° increased with increasing POSS content. The narrow and sharp reflection peaks of PCL phase showed perfect crystals.

The crystallinity of pure PCL and POSS/PCL hybrids were obtained by XRD analysis and the results were listed in Table I. In the hybrids, the crystallinity of PCL segment decreased with the increase of POSS content. The crystallinity of PP30 was lower than that of EP30, which indicated that the crystal formation of PCL segment was hindered by POSS. The reasons may be that incorporation of POSS nanocage into polymer chains prevented the formation of well-ordered chain regions and chain folding.[8]

Melting and Crystallization Behavior of POSS/PCL Hybrids and Pure PCL

Differential scanning calorimeter (DSC) heating and cooling scans of all samples were given in Figure 6. POSS/PCL hybrids were heated to 200 °C (100 °C for pure PCL) at 30 °C/min and kept at the temperature for 3 min to erase thermal history, and subsequently cooled to −90 °C at 5 °C/min and then heated to 200 °C (100 °C for pure PCL) at 10 °C/min. Figure 6(a) showed

Table I. The Molecular Weight and Molecular Weight Distribution of Pure PCL and POSS/PCL Hybrids

Samples	Initiator	ε-CL/-OH Molar ratio	$M_n \times 10^4$	$M_w \times 10^4$	M_w/M_n	POSS content (wt %)	Crystallinity (%)
EP10	EG	5	0.70	0.80	1.14	—	38.9
EP30	EG	15	1.17	1.57	1.34	—	36.3
EP120	EG	60	2.58	3.78	1.47	—	31.8
PP10	POSS	5	1.01	1.15	1.14	21.3	26.9
PP30	POSS	15	1.30	1.65	1.27	13.5	32.7
PP120	POSS	60	2.07	3.10	1.50	5.3	36.0

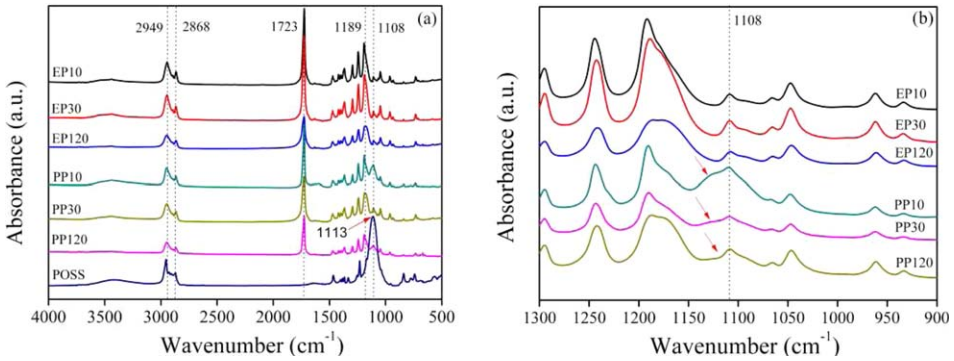

Figure 3. FTIR spectra of pure PCL and POSS/PCL hybrids: (a) 4,000–500 cm^{-1} and (b) 1,300–900 cm^{-1}. [Color figure can be viewed at wileyonlinelibrary.com.]

the cooling DSC curves of pure PCL and the hybrids. The curves showed that the onset crystallization temperature (T_0) of both PCL homopolymers and PCL segment of POSS/PCL hybrids moved to high temperature region with the increase of molecular weight. The higher the T_0 is, the easier polymers crystallize. This phenomenon illustrated that the crystallization of the PCL segment and PCL homopolymers became easier as molecular weight increased. The probable reasons were as follows. The factors that influenced crystallization included the free energy of formation of the critical nucleus and the free energy of transport at the interface liquid–crystal. When the molecular weight was low, the main influential factor was the free energy of formation of the critical nucleus, which showed a dependence on the molecular weight. Thus, the crystallization of the samples became easier with the increase of molecular weight due to a decrease in the free energy required for nucleation.[16] The Figure 6(a) also showed that the melt-crystallization temperature (T_{mc}) of the PCL segment were lower than that of corresponding homopolymer. The melt-crystallization peak of the POSS segment of was unobvious and disappeared with the increase of PCL content. In addition, The T_{mc} of the POSS segment (51.08 °C) was much lower than that

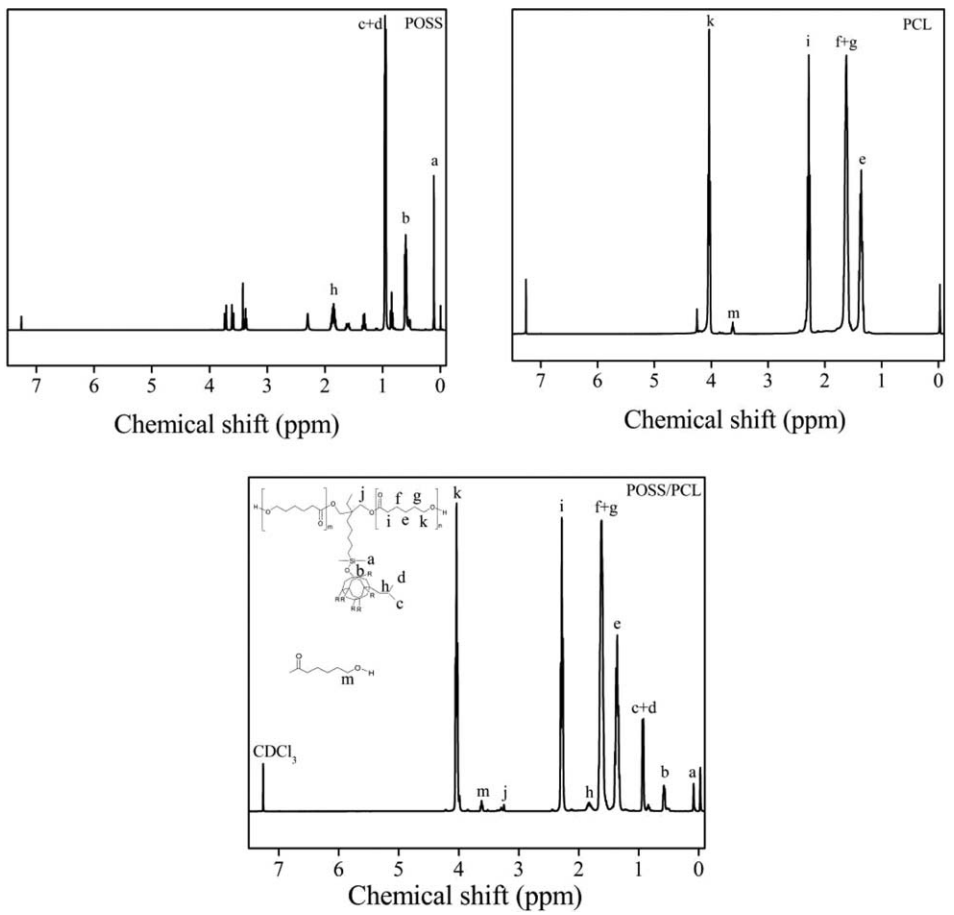

Figure 4. ^1H NMR spectra of POSS, PCL, and POSS/PCL hybrids.

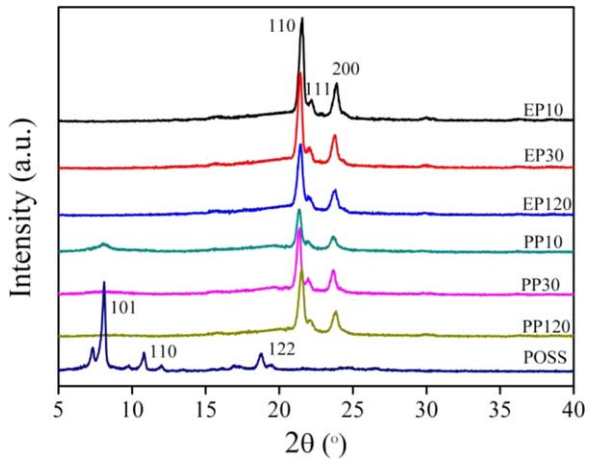

Figure 5. XRD traces of pure PCL, POSS/PCL hybrids, and POSS. [Color figure can be viewed at wileyonlinelibrary.com.]

of pure POSS (108.34 °C) (as shown in Supporting Information, Figure S1). These phenomena indicated that the crystallization of the PCL segment and the POSS segment were hampered mutually. The double melting peaks of PCL homopolymer and the PCL segment were observed in Figure 6(b), which were typical process including crystals melting, recrystallization, and remelting.[16] The shoulder peaks of the PCL segment were more evident than that of pure PCL, which suggested that the POSS segment impeded crystallization of the PCL segment.

Spherulite Morphology

The spherulite morphologies of pure PCL and POSS/PCL hybrids were studied by using hot-stage polarizing microscope (HSPOM) under isothermal crystallization at 40 °C. The HSPOM photos of pure PCL with various molecular weights were shown in Figure 7(a–c). For pure PCL, typical spherulites with Maltese cross birefringence patterns were observed. PP30 and PP120 [Figure 7(e–f)] also displayed the spherulite images with birefringence pattern. However, no spherulite could be observed in the POM image of PP10. To define crystal morphology of PP10, the crystal growth process was further observed. Figure 8(a–d) showed the crystal morphologies of PP10 at different periods. It was interesting that the crystal morphology of PP10 was quite different from the others (PP30 and PP120), which was similar to the shape of "snowflake". Strikingly, in the hybrids, higher content POSS had significant impact on crystallization of the PCL segment.

Non-Isothermal Crystallization Kinetics

The non-isothermal crystallization kinetics of pure PCL and POSS/PCL hybrids were performed by DSC. POSS/PCL hybrids were heated to 150 °C (100 °C for pure PCL) at 30 °C/min and kept the temperature for 3 min, and subsequently cooled to 0 °C at different rates of 6, 9, 12, and 15 °C/min. The DSC cooling curves of all samples at various rates were shown in Figure 9. The curves shifted to low temperature region and the width of melting-crystallization broadened as cooling rates increased. The reason may be as follow. The molecule had no enough time to form nuclei for crystallization under a fast cooling rate and the motion of molecular chain could not follow the cooling rate. Therefore, the curves moved to low temperature for the sake of nucleation.[17] Meanwhile, it required much more time for molecular chain packing.

Here, the non-isothermal crystallization behaviors of POSS/PCL hybrids and PCL homopolymers were investigated. The relative degree of crystallinity, X_T, as a function of crystallization temperature, T, can be defined as[17–19]:

$$X_T = \frac{\int_{T_0}^{T} (dH_C/dT)dT}{\int_{T_0}^{T_\infty} (dH_C/dT)dT} \quad (1)$$

where T_0 and T_∞ represent the onset and terminated crystallization temperatures of sample, respectively. dH_C is the enthalpy of crystallization. X_T versus T plots for PCL and POSS/PCL hybrids were shown in Supporting Information, Figure S2.

The crystallization time t was calculated using the following equation[17–19]:

$$t = \frac{T_0 - T}{\chi} \quad (2)$$

where T is the temperature at crystallization time t and χ is the cooling rate. Combining eqs. (1) and (2), the relative degree of crystallinity (X_t) is a function of crystallization time (t). That can be defined as following equation[18,19]:

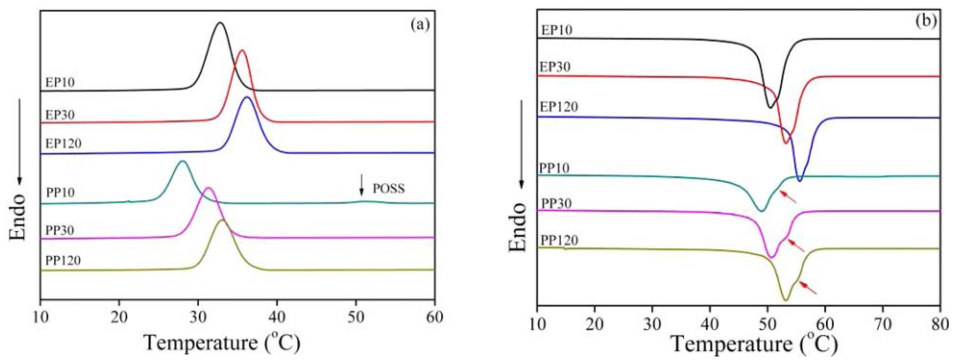

Figure 6. DSC curves of pure PCL and POSS/PCL hybrids. (a) Cooling scans and (b) the second heating scans. [Color figure can be viewed at wileyonlinelibrary.com.]

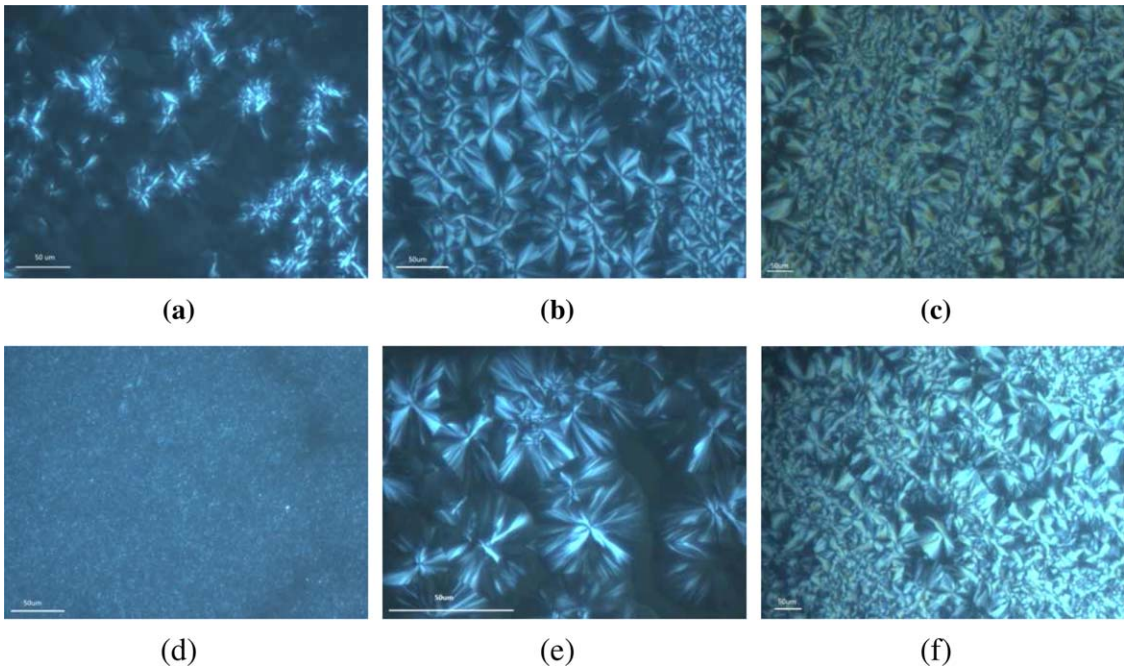

Figure 7. POM photographs of (a) EP10, (b) EP30, (c) EP120, (d) PP10, (e) PP30, and (f) PP120 spherulites observed under isothermal crystallization at 40 °C. [Color figure can be viewed at wileyonlinelibrary.com.]

$$Xt = \frac{\int_{t_0}^{t} (dH_C/dt)dt}{\int_{t_0}^{t_\infty} (dH_C/dt)dt} \quad (3)$$

where t_0 and t_∞ represent the onset and terminated time of melt crystallization, respectively. X_t versus t plots for PCL and POSS/PCL hybrids were shown in Supporting Information, Figure S3.

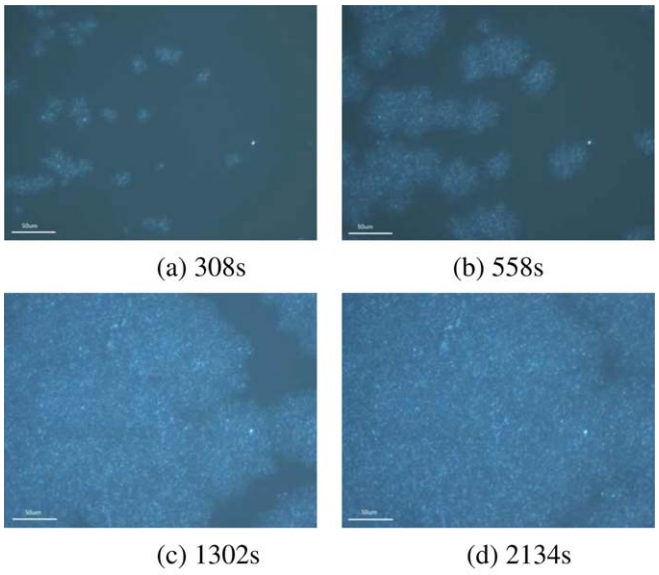

Figure 8. Crystal morphologies of PP10 during isothermal crystallization at 40 °C. [Color figure can be viewed at wileyonlinelibrary.com.]

The crystallization half-time ($t_{1/2}$) of all samples at different cooling rates were shown in Figure 10. The $t_{1/2}$ of pure PCL (EP10, EP30, and EP120) varied slightly, which suggested that the overall crystallization rate of PCL had no obvious change as molecular weight increased. For the same molecular weight, the $t_{1/2}$ of PP30 was much longer than that of EP30. As well known, incorporating POSS within polymeric architecture affected the crystallization rate of the matrix. On one hand, the steric hindrance of POSS core could reduce the molecular mobility of the matrix, which decelerated the rate of grain growth. However, POSS could act as the heterogeneous nucleating agent to accelerate the crystallization rate of the matrix.[20] In the present case, the overall crystallization rate decreased due to the incorporation of POSS. The content of POSS in PP30 was relatively low, some of the POSS molecule could molecular disperse in the matrix. The steric hindrance of POSS core reduced the molecular mobility of the PCL matrix. The $t_{1/2}$ for PP30 and PP1120 showed little difference, and they were much longer than that of PP10. For POSS/PCL hybrids with high content of POSS, some of the POSS molecule aggregated to form crystals and it could act as the heterogeneous nucleating agent to accelerate the crystallization rate of the matrix.[6,10,20]

The non-isothermal crystallization kinetics was further investigated by using the Mo equation, as follows[17,19]:

$$\log \chi = \log F(T) - \alpha \log t \quad (4)$$

where the parameter $F(T) = [K(T)/Z]^{1/m}$. The $K(T)$ refers to the Ozawa cooling function at temperature T and Z is Avrami crystallization rate constant. The physical meaning of $F(T)$ is that the value of cooling rate has to be chosen in a unit crystallization time when the measured system reaches a certain degree of crystallinity. α is ratio of Avrami exponent n to the Ozawa exponent m.

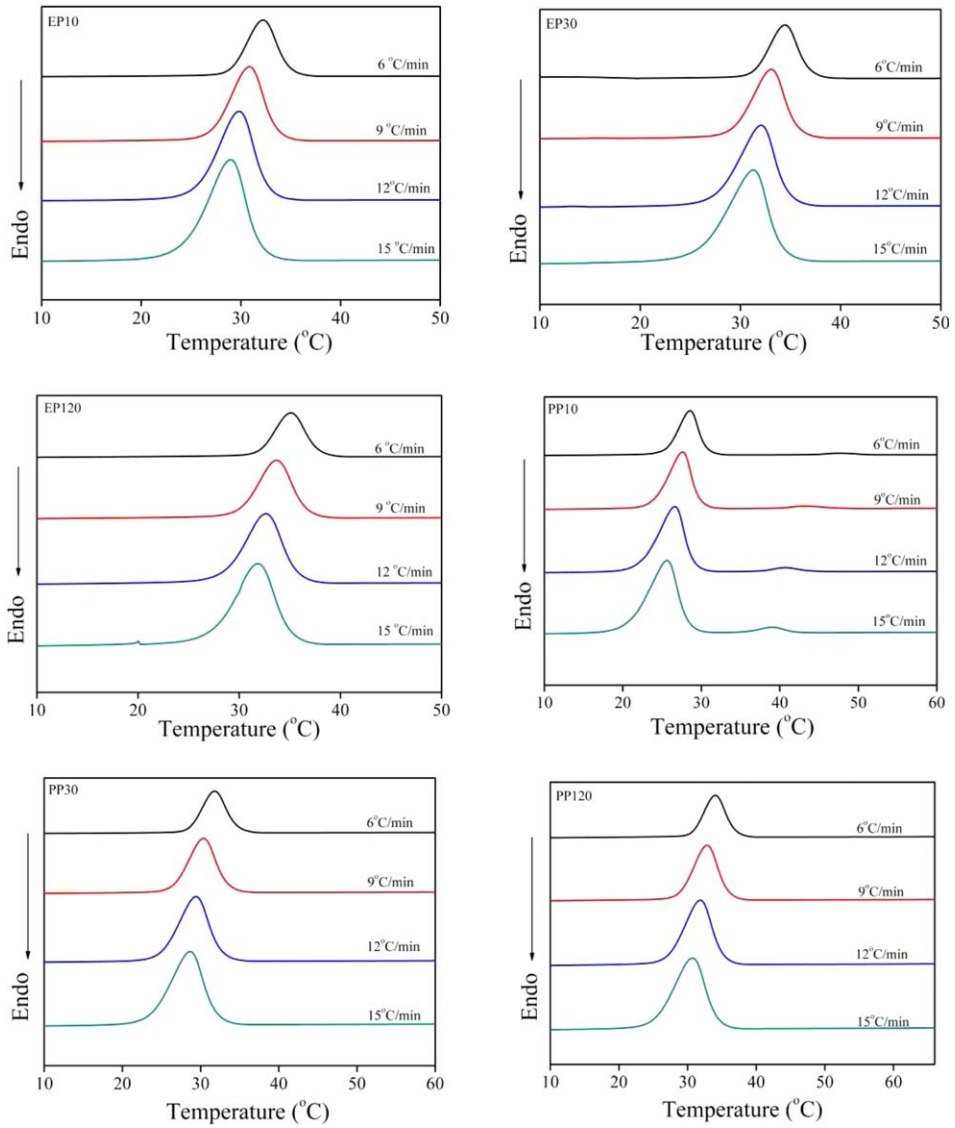

Figure 9. DSC cooling curves of pure PCL and POSS/PCL hybrids at various rates. [Color figure can be viewed at wileyonlinelibrary.com.]

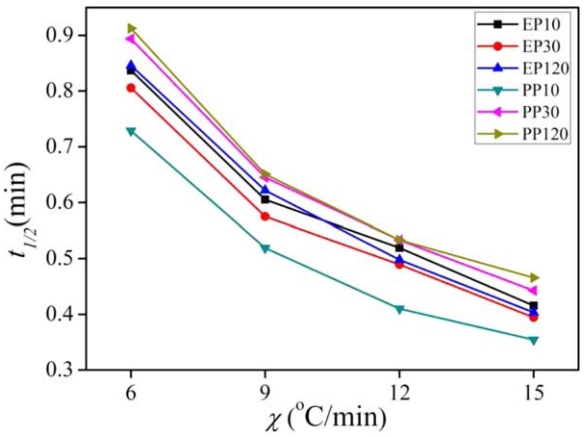

Figure 10. Crystallization half-time $t_{1/2}$ of pure PCL and POSS/PCL hybrids at different cooling rates. [Color figure can be viewed at wileyonlinelibrary.com.]

Combining eqs. (1–4), plots of log χ versus log t for pure PCL and POSS/PCL hybrids were given in Figure 11. The log χ and log t had a good linear relationship, indicating that the Mo equation could be used to analyze the non-isothermal crystallization process of pure PCL and POSS/PCL hybrids.[18,19] The value of α and $F(T)$ were estimated from the intercept and the slope of the plots, respectively. The parameters were listed in Table II. The Mo exponent value varied between 1.29 and 1.44, showing a little fluctuation for different samples and different degree of crystallinity. The $F(T)$ increased with the increase of relative degree of crystallinity in all samples. In certain relative degree of crystallinity, the larger the $F(T)$ is, the more slowly the polymers crystallize.[19] The value of $F(T)$ of PP30 was much larger than that of EP30, indicating that PCL segment of PP30 crystallized slowly than EP30. The value of $F(T)$ of PP30 and PP120 were much larger than that of PP10, showing that PP30 and PP120 crystallized slowly than PP10. These results were

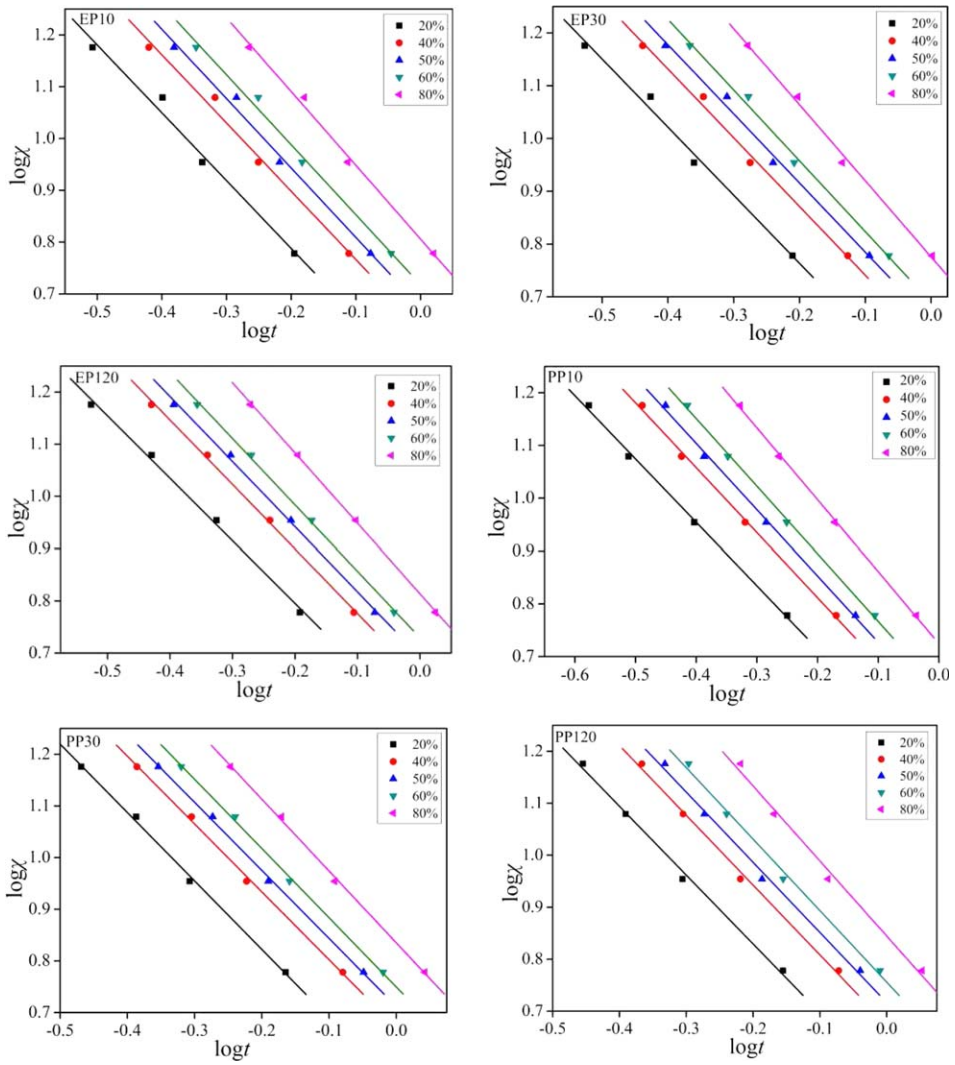

Figure 11. Plots of log χ versus log t for pure PCL and POSS/PCL hybrids at different degree of crystallinity. [Color figure can be viewed at wileyonlinelibrary.com.]

Table II. Values of $F(T)$ and α of Pure PCL and POSS/PCL Hybrids Obtained Using Mo Method

		Crystallinity (%)				
Samples	Parameters	20	40	50	60	80
EP10	*a*	1.31	1.32	1.34	1.35	1.42
	$F(T)$	3.36	4.31	4.73	5.22	6.40
EP30	*a*	1.29	1.30	1.31	1.34	1.44
	$F(T)$	3.20	4.08	4.50	4.89	5.97
EP120	α	1.20	1.24	1.25	1.27	1.35
	$F(T)$	3.60	4.49	4.93	5.36	6.51
PP10	α	1.20	1.23	1.25	1.28	1.36
	$F(T)$	2.98	3.68	3.40	4.35	5.30
PP30	α	1.32	1.31	1.32	1.34	1.39
	$F(T)$	3.61	4.69	5.15	5.62	6.84
PP120	α	1.32	1.34	1.35	1.38	1.44
	$F(T)$	3.67	4.70	5.21	5.70	6.99

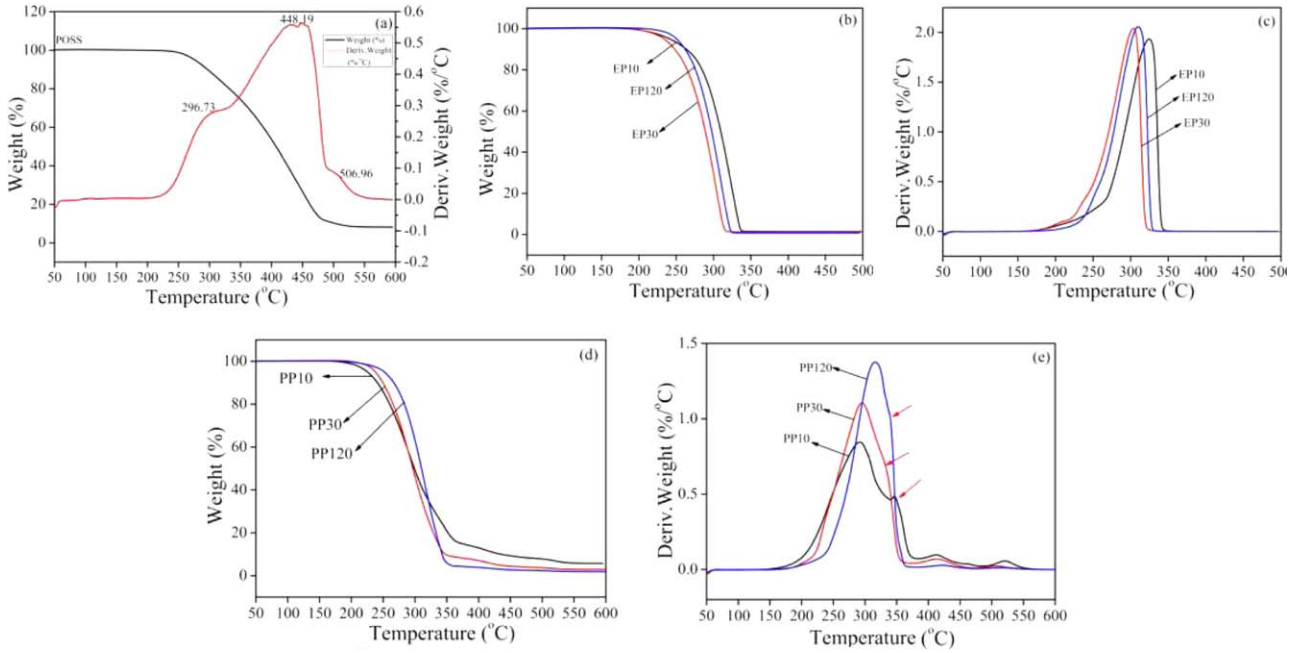

Figure 12. TG and DTG curves of POSS, pure PCL, and POSS/PCL hybrids. [Color figure can be viewed at wileyonlinelibrary.com.]

well coincident with those of $t_{1/2}$, which proved that Mo equation was successful in describing the non-isothermal crystallization process of POSS/PCL hybrids and PCL homopolymers.

Thermal Degradation

Thermal degradation behaviors of POSS, pure PCL, and POSS/PCL hybrids were studied by TGA. Figure 12 showed the thermogravimetry (TG) and differential thermogravimetry (DTG) curves of all samples. The degradation parameters, deriving from TGA curves, were summarized in Table III. The DTG trace of POSS [Figure 12(a)] showed a peak at 448.19 °C and two shoulders at 269.73 °C and 507.96 °C, respectively, which illustrated that the degradation process involved three consecutive mechanism. The weight loss at low temperature region probably resulted from the volatilization of POSS and the second and the third step probably attributed to the rupture of Si—C and Si—O—Si bonds.[21–25]

Table III. The Parameters of Thermal Degradation of Pure PCL, POSS/PCL Hybrids, and POSS

Samples		T_0 (°C)	$T_{5\%}$ (°C)	T_{max} (°C)	T_f (°C)
EP10		185.28	241.72	324.35	340.00
EP30		192.40	233.92	303.57	322.18
EP120		210.33	250.67	309.48	326.28
PP10	1st	174.70	225.63	291.79	548.06
	2nd			346.13	
	3rd			412.23	
	4th			520.02	
PP30	1st	199.00	238.00	295.65	538.03
	2nd			—	
	3rd			412.84	
	4th			506.14	
PP120	1st	186.66	251.12	316.43	544.62
	2nd			—	—
	3rd			422.46	
	4th			514.51	
POSS	1st	204.13	276.22	296.73	555.58
	2nd			448.19	
	3rd			506.96	

The TG and DTG curves of pure PCL [Figure 12(b,c)] displayed single step weight loss process in the 180–350 °C temperature range, mainly due to statistical rupture of the polyester chains.[25] The Figure 12(e) indicated that POSS/PCL hybrids underwent four-step weight loss process. According to the weight loss mechanism and weight loss temperature regions of POSS and pure PCL, the probable degradation process was as follows. For POSS/PCL hybrids, decomposition initially occurred through pyrolysis of ester bond, and then proceeded via volatilization of POSS, which resulted from the first step. Further decomposition occurred through thermal cracking of chemical bonds (Si—C, Si—O) of some residual POSS.

As seen in the Table III, the initial decomposition temperature (T_0) of pure PCL increased as molecular weight increased, whereas the T_0 of POSS/PCL hybrids increased first and then decreased. The temperature at 5% weight loss ($T_{5\%}$) of POSS/PCL hybrids increased with the increase of molecular weight, while the $T_{5\%}$ of pure PCL decreased first and then increased. The thermal degradation behaviors of POSS/PCL hybrids were very different from that of pure PCL. These phenomena showed that incorporation of POSS molecule affected thermal degradation of the hybrids. Additionally, for PP30, the T_0 value increased by 6.5 °C and the $T_{5\%}$ value increased by 4.6 °C compared with EP30. In addition, the thermal degradation temperature region of PP10 fell in a broader range. These results revealed that thermal stability of POSS/PCL hybrids enhanced by the introduction of POSS because POSS nanocage had higher thermal stability and it also constrained the movement of molecular chains.[9,26]

CONCLUSIONS

A series of POSS/PCL hybrids and pure PCL have been synthesized via open-ring polymerization in the presence of dibutyltin dilaurate. ^{1}H NMR and FTIR verified that POSS/PCL hybrids were synthesized successfully. The molecular weights of the polymers were determined by GPC and the measurement also showed relatively narrow molecular distribution of the samples. Crystal structures of POSS/PCL hybrids were analyzed by XRD and the results demonstrated that both POSS and PCL segment of POSS/PCL hybrids formed separated crystalline phase, except PP120 with low content of POSS in which only the PCL phase was formed.

The melting and crystallization behavior of POSS/PCL hybrids and pure PCL were carried on DSC. The results illustrated that the crystallization of the PCL segment and the POSS segment were hampered mutually.

The "snowflake" shape crystals of the highest POSS-containing PCL hybrid (PP10) were observed in POM images, which were quite different from crystal morphologies of the others.

The non-isothermal crystallization kinetics of POSS/PCL hybrids and pure PCL were explored using DSC at different cooling rates. Mo method was successfully described non-isothermal crystallization kinetics of POSS/PCL hybrids and pure PCL.

Thermal degradation of POSS/PCL hybrids and pure PCL were studied by TGA. The degradation of POSS/PCL hybrids proceeded by four-step while pure PCL degraded by a single step. The initial decomposition temperature and the temperature at 5% weight loss of PP30 were higher than that of corresponding homopolymer.

ACKNOWLEDGMENTS

This work was supported by National Natural Science Foundation of China (51403084), the Natural Science Foundation of Jiangsu Province (BK20130142), the Key Laboratory of Food Colloids and Biotechnology, Ministry of Education, Jiangnan University (JDSJ2013-05), the Open Project Program of Key Laboratory of Yarn Forming and Combination Processing Technology of Zhejiang Province (Jiaxing University) (MTC2014-008), the Fundamental Research Funds for the Central Universities of Jiangnan University (JUSRP51417B), and the Priority Academic Program Development of Jiangsu Higher Education Institutions.

REFERENCES

1. Woodruff, M. A.; Hutmacher, D.,W. *Prog. Polym. Sci.* **2010**, *35*, 1217.
2. Choi, J. H.; Jung, C. H.; Hwang, I. T.; Choi, J. H. *Nucl. Instrum. Meth. A* **2012**, *287*, 100.
3. Lee, K. M.; Knight, P. T.; Chung, T.; Mather, P. T. *Macromolecules* **2008**, *41*, 4730.
4. Pert, C. B.; Snowman, A. M.; Snyder, S. H. *Polym. Int.* **2014**, *63*, 479.
5. Huitron-Rattinger, E.; Ishida, K.; Romo-Uribe, A.; Mather, P. T. *Polymer* **2013**, *54*, 3350.
6. Liu, Y. H.; Yang, X. T.; Zhang, W. A.; Zheng, S. X. *Polymer* **2006**, *47*, 6814.
7. Mirmohammadi, S. A.; Imani, M.; Uyama, H.; Atai, M. *Int. J. Poly. Mater.* **2014**, *63*, 624.
8. Mirmohammadi, S. A.; Imani, M.; Uyama, H.; Atai, M. *J. Poly. Res.* **2013**, *20*, 1.
9. Fernández, M. J.; Fernández, M. D.; Cobos, M. *RSC Adv.* **2014**, *4*, 21435.
10. Mya, K. Y.; Gose, H. B.; Pretsch, T.; Bothe, M.; He, C. *J. Mater. Chem.* **2011**, *21*, 4827.
11. Alvarado-Tenorio, B.; Romo-Uribe, A.; Mather, P. T. *Macromolecules* **2011**, *44*, 5682.
12. Kim, B. S.; Mather, P. T. *Macromolecules* **2002**, *35*, 8378.
13. Goffin, A. L.; Duquesne, E.; Moins, S.; Alexandre, M.; Dubois, P. *Europ. Polym. J.* **2007**, *43*, 4103.
14. Chan, S. C.; Kuo, S. W.; She, H. S.; Lin, H. M.; Lee, H. F. *J. Poly. Sci. A: Poly. Chem.* **2007**, *45*, 125.
15. Gu, X.; Jian, W.; Mather, P. T. *Biomacromolecules* **2011**, *12*, 3066.
16. Liu, Q.; Shyr, T. W.; Tung, C. H.; Deng, B.; Zhu, M. *Fiber. Polym.* **2011**, *12*, 848.
17. Xing, P.; Dong, L.; An, Y.; Feng, Z. L. *Europ. Polym. J.* **1997**, *33*, 1449.

18. Choi, J.; Chun, S.; Kwak, S. *Macromol. Chem. Phys.* **2006**, *207*, 1166.
19. Liu, Q.; Deng, B.; Tung, C. H.; Zhu, M.; Shyr, T. W. *J. Polym. Sci. B: Polym. Phys.* **2010**, *48*, 2288.
20. Fu, B. X.; Yang, L.; Somani, R. H.; Zong, S. X.; Hsiao, B. S. *J. Polym. Sci. B: Polym. Phys.* **2001**, *39*, 2727.
21. Mantz, R. A.; Jones, P. F.; Chaffee, K. P.; Lichtenhan, J. D.; Gilman, J. W.; Ismail, I. M. K.; Burmeister, M. *J. Chem. Mater.* **1996**, *8*, 1250.
22. Fina, A.; Tabuani, D.; Carniato, F.; Frache, A.; Boccaleri, E.; Camino, G. *Thermochim. Acta* **2006**, *440*, 36.
23. Bolln, C. *Chem. Mater.* **1997**, *9*, 1475.
24. Cai, L.; Foster, C. J.; Liu, X.; Wang, S. *Polymer* **2014**, *55*, 3836.
25. Persenaire, O.; Alexandre, M.; Degée, P.; Dubois, P. *Biomacromolecules* **2001**, *2*, 288.
26. Lee, Y. J.; Kuo, S. W.; Su, Y. C.; Chen, J. K.; Tu, C. W.; Chang, F. C. *Polymer* **2004**, *45*, 6321.